RESEARCH ARTICLE

Editorial Process: Submission:07/20/2022 Acceptance:11/10/2022

Novel Derivatives of Tetrahydrobenzo (g) Imidazo[α-1,2] Quinoline Induce Apoptosis Via ROS Production in the Glioblastoma Multiforme Cells, U-87MG

Fatemeh Mostafavi Hosseini[1], Maryam Ashourpour[1], Salman Taheri[2], Masoumeh Tavakoli-Yaraki[3], Siamak Salami[4], Zahra Shahsavari[4]*, Faranak Kazerouni[1]

Abstract

Background: Despite newer therapeutic approaches against glioblastoma multiforme (GBM), the severely poor prognosis and treatment resistance are still disadvantages that slow down the patient's recovery process. Consistent with the need to develop more effective and optimized therapies to control GBM cell growth, the effects of a new series of tetrahydrobenzo(g)imidazo[α-1,2]quinolone derivatives on GBM cell growth and the underlying mechanism is investigated in the current study. **Methods:** U-87MG cell line, glioblastoma multiforme and normal skin fibroblast cell line, AGO1522 were used to study the anticancer effects of 5 derivatives of tetrahydrobenzo(g)imidazo[α-1,2]quinolone and paclitaxel as a standard drug. The cytotoxic effect on cell growth was assessed using the MTT assay. Annexin V FITC staining and PI staining were applied to detect apoptosis and cell cycle distribution using flow cytometry. The extent of reactive oxygen species (ROS) formation was assessed using the fluorescent probe 7-dichlorofluorescin diacetate and caspase-3 activity using the colorimetric assay kit. **Results:** Among the 5 derivatives of tetrahydrobenzo(g) imidazo[α-1,2]quinolone, the 5c derivative (5-(6-bromo-2-chloroquinolin-3-yl)-9a-hydroxy-8,8-dimethyl-4-Nitro-2,3,5,5a,7,8,9,9a-octahydroimidazo[α-1,2]quinoline-6(1H)) showed the strongest cytotoxic effect on U-87MG cells in a time and Dose-dependent manner compared to the other derivatives and paclitaxel. The IC_{50} (11.91 M) of the 5c derivative induced apoptosis accompanied by a significant increase in sub-G1 and super-G2 phases of U-87MG cells. The increased level of cellular ROS and caspase 3 activity after treatment of U-87MG cells with 5c derivative was significant compared to untreated cells. **Conclusion:** Our data provide insights into the potent anticancer effects of the 5c-derivative of tetrahydrobenzo(g)imidazo[α-1,2]quinolone on GBM cells via the caspase-dependent apoptotic pathway, which may merit further attention.

Keywords: Glioblastoma multiforme- imidazoquinoline- apoptosis- ROS- reactive oxygen species

Asian Pac J Cancer Prev, **23 (11)**, 3885-3893

Introduction

Based on the WHO classification, glioblastoma multiform (GBM) is a high-grade, aggressive, and undifferentiated glioma that accounts for up to 50% of gliomas worldwide with a 5-years survival rate of less than 6% (Hanif et al., 2017; Elsakka et al., 2018; Shergalis et al., 2018). The tumor incidence rate includes all age ranges with at least pronounced peaks in late adulthood and between the ages of 55 and 60 (Huang et al., 2017). GBM's low survival rate may be due in part to its invasive nature, resistance to therapy, and ability to invade the brain parenchyma (Stylli, 2020). The therapeutic approaches of GBM are based on surgical resection together with a combination of alkylating agent-based chemotherapy and radiotherapy. Among chemotherapy drugs, temozolomide (TMZ) is the most widely used and effective agent, which is routinely used in GBM patients as an adjuvant to radiotherapy to relieve patients' symptoms (Hu et al., 2020). Despite the effectiveness of TMZ in increasing patient survival rate, producing many side effects and chemoresistance to apoptosis are prominent disadvantages of TMZ administration that result in GMB being a cancer with poor prognosis and high mortality rate (Hanif et al., 2017). Accordingly, efforts are underway to develop more efficient therapeutic approaches to improve patient prognosis and reduce disease-related morbidity (Stylli, 2020). Imidazoquinolines are heterocyclic skeletons

*[1]Department of Laboratory Medicine, Faculty of Paramedical Sciences, Shahid Beheshti University of Medical Sciences, Tehran, Iran. [2]Chemistry & Chemical Engineering Research Center of Iran, Tehran, I.R., Iran. [3]Department of Biochemistry, School of Medicine, Iran University of Medical Sciences, Tehran, Iran. [4]Department of Clinical Biochemistry, Faculty of Medicine, Shahid Beheshti University of Medical Sciences, Tehran, Iran. *For Correspondence: z.shahsavari@sbmu.ac.ir. Fatemeh Mostafavi Hosseini and Maryam Ashourpour have equal contribution in this study.*

generated by the fusion between the 5-membered imidazole ring and the benzopyridine ring, quinolone (Bazin et al., 2018). Evidence indicates that imidazoquinolines exhibited antibacterial, antiparasitic, antiallergic, and anxiolytic effects (Smith et al., 2003; Schwartz et al., 2009). Recently, the antiproliferative properties of imidazoquinolines have attracted considerable interest, making these compounds promising candidates for tumor cell growth control (Courbet et al., 2017). Accordingly, imiquimod, known as Aldara or R-837, has been shown to modify immune cell responses by acting as a TLR7 agonist and is a Food and Drug Administration -approved therapeutic for basal cell carcinoma and genital warts (Vacchelli et al., 2012). Gardiquimod has been shown to suppress cancer cell proliferation by inducing apoptosis and inhibiting metastasis (Zou et al., 2015). Furthermore, it was shown that treatment with imidazoquinoline induced the infiltration of T-cell lymphocytes and the production of pro-inflammatory cytokines even in established mouse renal cell carcinoma (RCC) tumors, induced apoptosis and suppressed tumor cell proliferation(Kauffman et al., 2012). Despite promising evidence for the antiproliferative effects of imidazoquinoline in cancer cells, little is known about the precise role of imidazoquinoline derivatives and the mechanism underlying their action on various types of cancer. Accordingly, the current study aims to investigate the possible effects of imidazoquinoline and its derivatives on the induction of apoptosis, cell cycle distribution, caspase-3 activity and ROS generation in human U-87MG glioblastoma cells. The results of this study may provide insights into the efficacy of imidazoquinoline as a potential anticancer agent for future GBM therapeutic approaches.

Materials and Methods

Reagents

RPMI 1640 medium, Dulbecco's modified eagle medium low glucose (DMEM/Low Glucose), fetal bovine serum (FBS), penicillin-streptomycin and trypsin- EDTA were purchased from Gibco (Grand Island, NY, USA). Propidium iodide (PI), DMSO, 3-(4,5-dimethyl-2-thiazolyl)-2,5-diphenyl-2H-tetrazolium bromide (MTT) and 2',7'-dichlorofluorescein diacetate (DCF-DA) were bought from Sigma-Aldrich, (Munich, Germany). Annexin V-FITC/PI apoptosis kit was obtained from Biolegend (San Diego, USA). The Caspase-3 Fluorometric Assay Kit was bought from BioVision, Inc. (Milpitas, CA, USA).

Cell culture

The human glioblastoma cell line, U-87MG and the normal human skin fibroblast cell line, AGO1522 were obtained from the National Cell Bank of Iran (Pasteur Institute of Iran, Tehran). The cells were cultured in 25 cm^2 cell culture flasks and maintained under standard sterile conditions. U-87MG cells were cultured in RPMI-1640 and AGO1522 cells were cultured in low-glucose DMEM with medium supplemented with 10% FBS, 100 U/ml penicillin and 100 µg/ml streptomycin at 37°C, 5% CO_2 and cultivated in a humidified atmosphere. Fresh medium was provided to the cells every 2-3 days and when the cells reached 70% confluency, the cells were harvested using trypsin (0.25%)-EDTA (0.02%). Collected cells were used fresh or frozen and stored in liquid nitrogen for subsequent experiments. The compounds were dissolved in DMSO at concentrations of 10,000 M and stored in the dark at -20°C. For treatment, imidazoquinoline derivatives were further diluted in medium to final concentrations.

Cell viability assay

To determine the proliferative capacity of imidazoquinoline derivatives on the U-87MG cells, a MTT assay was used. The structure of the imidazoquinoline derivatives (5 a–e) studied in this study is shown in Figure 1 and their molecular weight and characteristics are shown in Table 1. The MTT assay is a standard colorimetric assay used for the assessment of cell viability based on the activity of reducing mitochondrial dehydrogenase enzymes of viable cells. After tetrazolium dye reduction, a violet color is produced that is proportional to the rate of viable cells. Briefly, U-87MG cells (7.5×10^3 cells/well) were seeded in 96 wells cell culture plate and after 24 h incubation, the cells were stimulated with different concentrations of imidazoquinoline derivatives and paclitaxel as standard drug. The concentrations of imidazoquinoline derivatives and paclitaxel were 3, 6.25, 12.5, 25, 50, 100 µM and the cells were incubated for 24 and 48 hours. The MTT solution (5 mg/ml in PBS) was added to each well and after 4 hours of incubation, the supernatant of each well was removed and replaced with DMSO, which formed dissolved purple formazan crystals. The absorbance of each well was measured at 570 nm with a microplate reader (BioTek Synergy HT, Winooski, VT, USA). Based on the comparison of the absorbance of treated and untreated cells, the viability rate was calculated.

Assessment of Apoptosis

To assess the rate of apoptotic cells, the AnnexinV-FITC/PI double staining method using flow cytometry was applied according to the manufacturer's instructions. The method is based on the detection of phosphatidylserine exposed on the surface of apoptotic cells. Briefly, U-87MG cells (6 x 10^5 cells/well) were seeded in 6 wells plate and after 24 hours of incubation, the cells were treated with 5c derivative at a final concentration of 11.91 µM for 24 hours. The cells were washed twice with PBS and after trypsinization and centrifugation, the cells were washed with cold PBS and suspended in 300 µL of Annexin V binding buffer. Then 5 µl of annexin V-FITC and 5 µl of propidium iodide were added and mixed homogeneously. The cells were incubated at room temperature for 15 minutes in the dark and the cells were transferred to a FACSCalibur flow cytometry tube (BD FACSCalibur flow cytometer, USA) and analyzed using FlowJo V. 10 software. The Annexin V positive, PI negative cells represented early apoptotic cells, and double positive of Annexin V and PI indicated late apoptotic cells.

Cell cycle analysis

PI staining was used to assess DNA content and cell cycle distribution using flow cytometry. Based on

the instructions, U-87MG cells (6 x 10^5 cells/well) were seeded in 6 wells cell culture plate and after 24 h incubation, the cells were treated with 11.91 µM 5c-derivative for 24 h. The trypsin-EDTA solution was used to detach cells at 37°C for 2 min and trypsin activity was stopped using RPMI-1640 medium. After appropriate washing with PBS, the cells were suspended in 300 µL of PBS and fixed in 700 µL of cold 70% ethanol for 1 hour. Finally, after washing, the cell pellets were suspended in 1 ml sodium citrate (0.1%) containing 0.05 mg PI and 50 µg RNase for 30 min at room temperature in the dark. Accumulation of cells in the sub-G1 region of DNA distribution histograms indicated DNA-damaged cells and is considered a hallmark of apoptosis. The percentage of cells in the sub-G1, G0/G1, S and G2/M phases was analyzed by flow cytometry (BD FACS Calibur flow cytometer, USA) and FlowJo software V.10.

Reactive Oxygen Species (ROS) Assay

DCFH-DA was used as a fluorescence probe to determine the intracellular ROS amount. An increase in intracellular ROS can be associated with the occurrence of apoptosis, and in the presence of ROS, DCFH is oxidized to highly fluorescent DCF, which is detected with a fluorimeter. Based on the instructions, cells (6 x 10^5 cells/well) were seeded in 6 wells plate and after 24 h incubation treated with 11.91 µM 5c-derivative for 12 h. The cells were exposed to the fluorescent probe DCFH-DA (final concentration: 10 µM) in serum-free cell culture medium for 30 min at 37°C in the dark. After washing twice with culture medium (RPMI 1640), 1 x 10^4 cells were bulked out for analysis using a fluorescent microplate reader (BioTek Synergy HT, Winooski, VT, USA).

Measurement of Caspase-3 Activity

The level of caspase-3 activity was detected using the Caspase-3/CPP32 Fluorometric Assay Kit. To achieve this, U-87MG cells were treated with 11.91 µM 5c derivative for 12 hours and 0.5-2 x 10^5 cells were resuspended in 50 µL of chilled cell lysis buffer and incubated on ice for 10 minutes. After determination of protein concentration using the Bradford method, 50 µl of 2X reaction buffer containing 10 mM DTT was added to the cells and the cells were incubated at 37°C for 2 hours with 50 µM DEVD-AFC substrate. DEVD-AFC is a synthetic substrate for determining caspase-3 activity. Free AFC content using a fluorescent microplate reader (BioTek Synergy HT, Winooski, VT, USA) on the excitation filter at 400 nm and an emission filter at 505 nm.

Statistical analysis

To determine statistical differences between groups, Student's t-test or one-way nonparametric analysis of variance (ANOVA) with Dennet's and Tukey's post-hoc tests for multiple comparisons were used. Data are presented as mean deviation (SD) and all experiments were performed in triplicate and replicated at least three times to determine specificity and accuracy. The IC_{50} values of imidazoquinoline derivatives (half-maximal inhibitory concentration) were calculated. P values less than 0.05 were considered statistical significance. Data analysis and statistical calculations were performed using statistical software Graph Pad Prism Version 6 (CA, USA).

Results

Imidazoquinoline derivatives inhibit U-87MG cells proliferation in a concentration- and time-dependent manner

To determine the possible effects of imidazoquinoline derivatives on the viability of human glioblastoma cells (U-87MG) and human skin fibroblasts (AGO1522), cells at different concentrations (3, 6.25, 12.5, 25, 50, 100 µM) derivatives treated with imidazoquinoline and paclitaxel as standard drug were administered for 24 and 48 hours and cell viability was measured using the MTT assay. Based on data demonstrating that U-87MG cell viability was significantly reduced in a time- and concentration-dependent manner after treatment with imidazoquinoline derivatives. As shown in Figure 2, imidazoquinoline derivatives reduced the viability of U-87MG after 24 (Figure 2a) and 48 (Figure 2b) hours of incubation. A comparison of the IC_{50} values of imidazoquinoline derivatives after 24 and 48 hours of incubation showed that the cytotoxic effect was more pronounced after 48 hours of incubation. As shown in Table 2, the IC_{50} values of imidazoquinoline derivatives on U-87MG cells are significantly lower compared to the IC_{50} values of paclitaxel at both time intervals. It was also shown that the 5c derivative had the lowest IC_{50} value after 24 and 48 hours of incubation. Accordingly, the 5c derivative with a concentration of 11.91 µM and an incubation time of

Table 1. Tetrahydrobenzo (g) Imidazo[α-1,2] Quinolone Derivatives Characteristics

		Molecular weight (g/mol)
5a	5- (2-chloro quinolin-3-yl) -10b-hydroxy-4-nitro-1,2,3,5,5a,10b-hexahydro-6H-imidazo [1,2-a] indeno [2,1-e] pyridin-6-one	412.41
5b	5- (2-chloroquinolin-3-yl) -9a-hydroxy-8,8-dimethyl-4-nitro-2,3,5,5a,7,8,9,9a octahydroimidazo [1,2-a] quinolin-6 (1H) -one	406.44
5c	5-(6-bromo-2-chloroquinolin-3-yl)-9a-hydroxy-8,8-dimethyl-4-nitro-2,3,5,5a,7,8,9,9a-octahydroimidazo[1,2-a]quinolin-6(1H)-one	485.34
5d	5-(2-chloro-6-methylquinolin-3-yl)-9a-hydroxy-8,8-dimethyl-4-nitro-2,3,5,5a,7,8,9,9a-octahydroimidazo[1,2-a]quinolin-6(1H)-one	420.47
5e	5-(9-chloro-4-nitro-1,2,3,5-tetrahydrobenzo[g]imidazo[1,2-a] [1,8] naphthyridin-5-yl) -6-hydroxypyrimidine-2,4 (1H, 3H) -dione	428.79

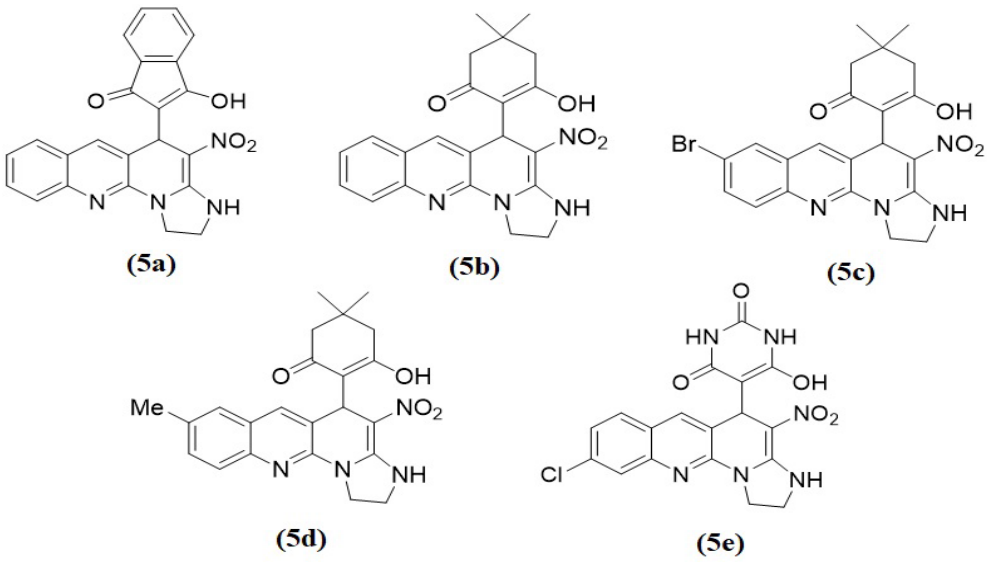

Figure 1. Structures of Novel Tetrahydrobenzo (g) Imidazo[α-1,2] Quinolone Derivatives. The chemical structure of 5 different derivatives of this compound is shown separately.

24 hours was used as the optimal concentration and time in the subsequent experiments. The cytotoxic effects of imidazoquinoline derivatives on AGO1522 cells were significantly less after 24 (Figure 2c) and 48 (Figure 2d)

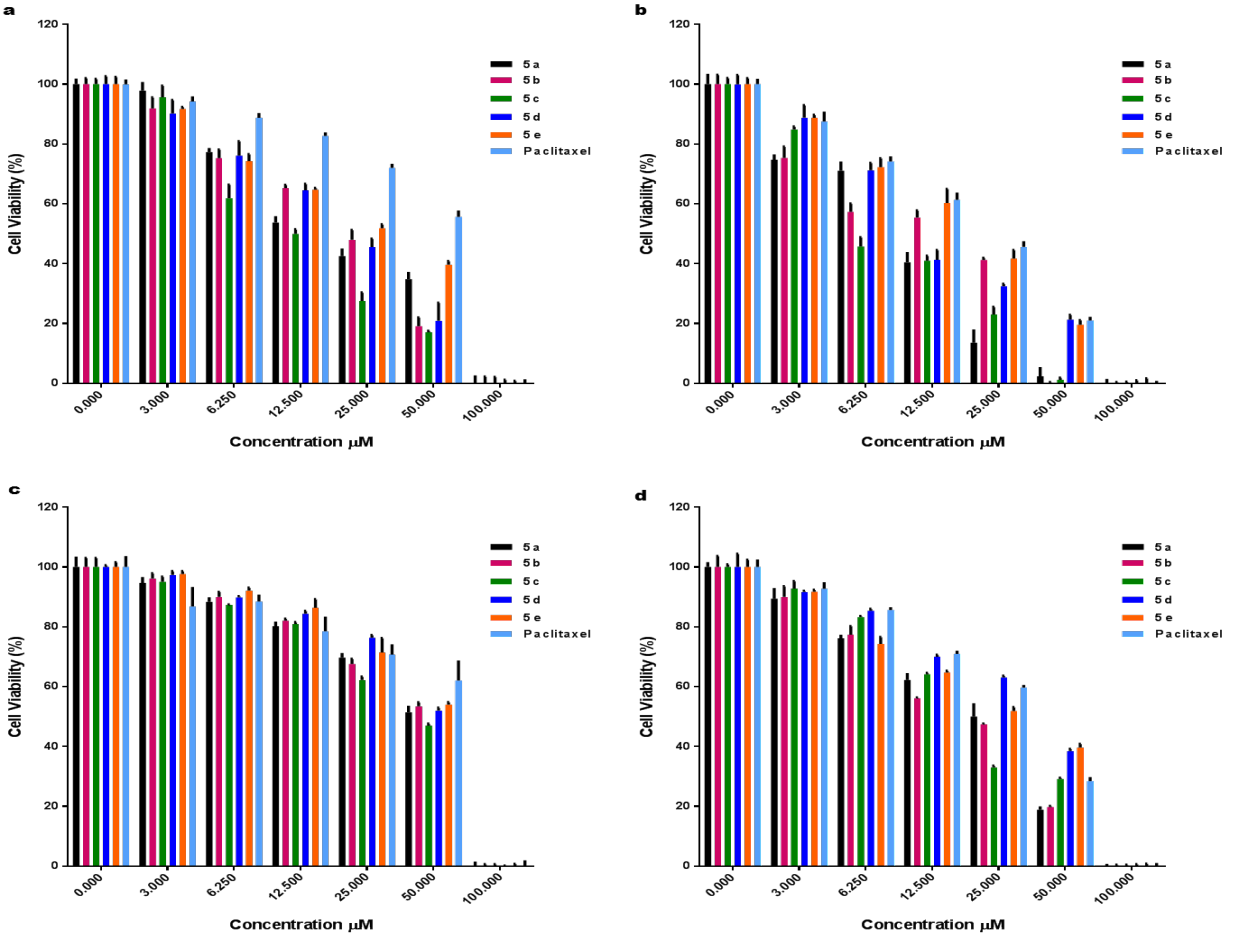

Figure 2. The cytotoxic effects of Tetrahydrobenzo (g) imidazo[α-1,2] quinolone derivatives and Paclitaxel in U-87MG and AGO1522 cells. Human glioblastoma cells (U-87MG) and normal human skin fibroblast cell line (AGO1522) were treated with 3, 6.25, 12.5, 25, 50, 100 μM of imidazoquinoline derivatives (5a-5e) and Paclitaxel for 24 and 48 hours and the rate of viable cells following treatments was detected using MTT assay. A dose-dependent reduction of viable U-87MG cells following 24 hours (a) and 48 hours (b) was detected. The percentages of viable AGO1522 cells after 24 hours (c) and 48 hours (d) is shown. Data represent mean±SD of three separate experiments and the statistical differences between treated and untreated groups were analyzed by ANOVA.

Table 2. IC_{50} Values of Novel Tetrahydrobenzo (g) Imidazo[α-1,2] Quinolone Derivatives and Paclitaxel in U-87MG and AGO-1522 Cells after 24 and 48 hours of Incubation.

	U-87MG		AGO1522	
	24 hours	48 hours	24 hours	48 hours
5a	18.38 ± 0.83*	9.40 ± 0.90	38.80 ± 0.75	18.85 ± 0.94
5b	18.94 ± 0.92	10.84 ± 0.92	39.82 ± 0.94	17.88 ± 0.76
5c	11.91 ± 0.85	7.72 ± 0.65	34.10 ± 0.85	18.73 ± 0.83
5d	18.54 ± 0.93	12.89 ± 0.96	43.45 ± 0.79	28.44 ± 1.07
5e	22.62 ± 0.84	16.26 ± 1.03	42.99 ± 0.89	22.86 ± 0.95
Paclitaxel	17.42 ± 0.85	42.18 ± 0.78	42.93 ± 1.42	25.79 ± 1.09

*Data shown are mean ± SD of triplicate samples.

hours of incubation compared to the U-87MG cells.

5c derivative induces apoptosis in U-87MG glioblastoma cells

To determine whether the cytotoxic effect of the 5c derivative on U-87MG glioblastoma cells was correlated with the induction of apoptosis, the Annexin V/PI staining procedure was used. Based on the data, treatment with 11.91 µM 5c-derivative for 24 hours significantly induced both early and late apoptosis. The flow cytometric histograms of the effects of the 5c derivative on the apoptotic cell percentages of U-87MG-unexposed negative cells and U-87MG treated cells are shown in Figure 3a. It was found that the percentage of early and late apoptotic cells was significantly increased after treatment with 11.91 µM 5c derivative compared to the untreated U-87MG cells ($P<0.001$). In addition, a significant reduction in viable cell percentages was demonstrated after treatment of U-87MG cells with 5c derivative compared to the untreated U-87MG cells

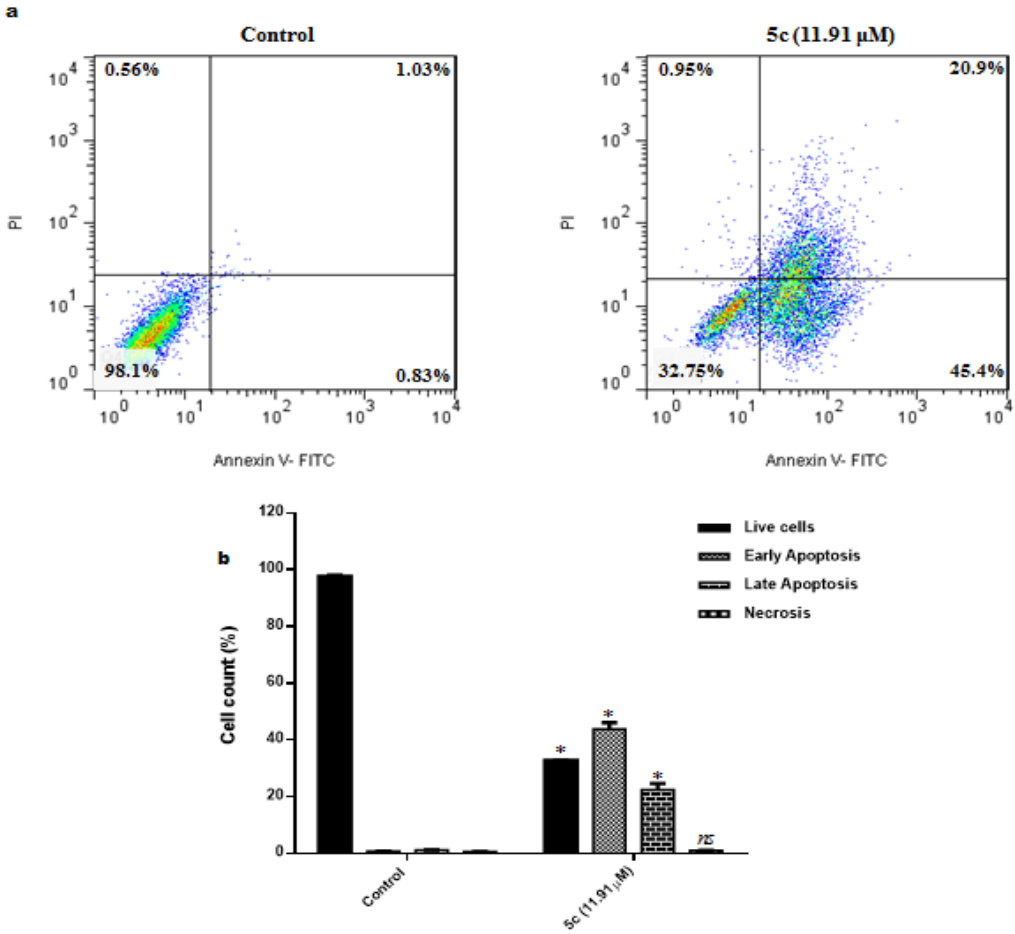

Figure 3. 5c Derivative Induced Apoptosis in U-87MG Cell Line. To evaluate the rate of apoptosis, the annexin-V and PI staining was applied and the percentages of cells were determined using flow cytometry. The flow cytometry histograms (a) indicate the un-treated U-87MG cells and the treated U-87MG cells with 11.91 µM of 5c derivative for 24 hours. Also b section represents percentages of cells at the early (stained with annexin V only) and late (stained with both annexin V and PI) apoptosis stages following treatment. Data are representative of three independent experiments. *$P<0.05$ denotes a mean significantly different from untreated cells, ns not significantly different from untreated cells.

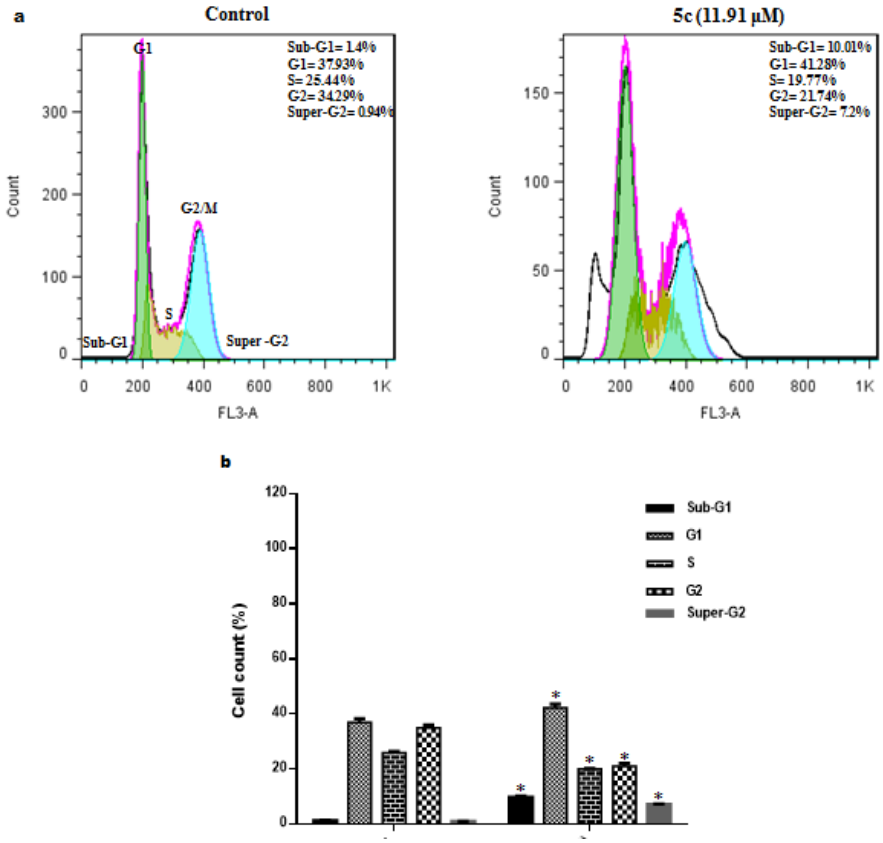

Figure 4. 5c Induces Cell Cycle Arrest in U-87MG Cells.

(Figure 3b, P<0.001).

5c induces S and G2/M cell cycle arrests in U-87MG glioblastoma cells

It is well documented that a change in cell cycle distribution and accumulation of cells in the sub-G1 phase is a hallmark of apoptosis. PI staining was used to determine the cell cycle pattern of U-87MG cells exposed to 11.91 µM 5c derivative after 24 hours of incubation. The pattern of cell cycle distribution is shown in Figure 4a. Based on the data, a significant increase in the percentage of cells in the sub-G1 fraction was observed after treatment. The cell population in G1 phase increased to 41%, which was accompanied by a decrease in S and

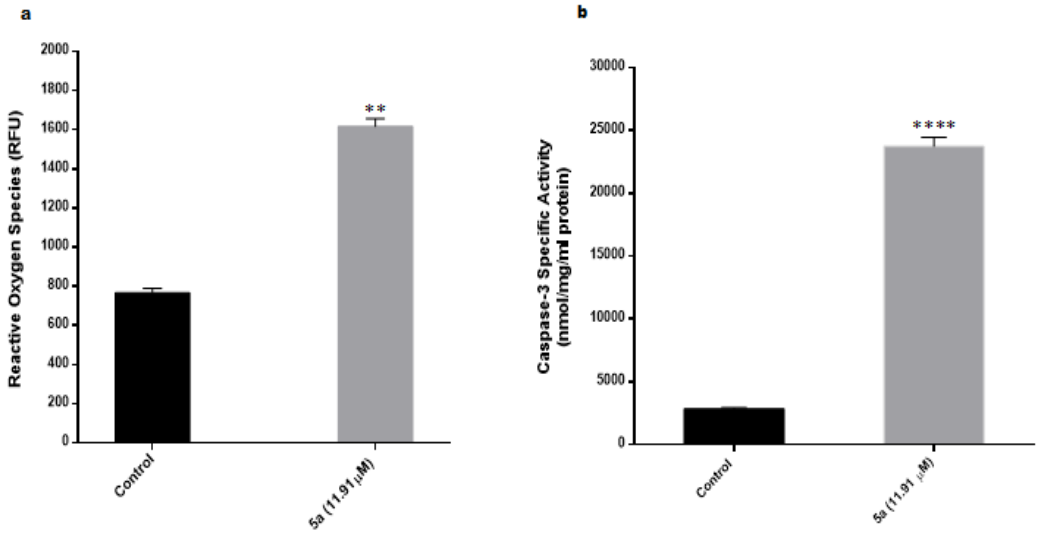

Figure 5. The Effects of 5c Derivative on Cellular Level of ROS and Caspase 3 Activity in U-87MG Cells. The ROS measurement using DCFH-DA florescent probe and the level of caspase 3 activity was detected using the Caspase-3/CPP32 Fluorometric Assay Kit. The cellular level of ROS following treatment of U-87MG cells with 11.91 µM of 5c derivative for 24 hours was increased (a). Also, the caspase 3 activity following treatment of U-87MG cells with 11.91 µM of 5c derivative for 24 hours was elevated significantly (b). Data points represent RFU (relative fluorescence unit) of three independent experiments for ROS detection. **P<0.01 and ****P<0.0001 denotes a mean significantly different from untreated cells.

G2 phases in the 11.91 μM 5c-derivative treated U-87MG cells (Figure 4b). The results showed that administration of 5c derivatives induced post-G1 arrest and apoptosis in human glioblastoma cells.

The elevation of ROS level following 5c-induced apoptosis

To determine whether treatment of U-87MG cells with 5c derivatives resulted in changes in intracellular ROS levels, DCFH-DA fluorescence intensity was assessed using a fluorimeter. After treating the cell with 5c-derivative (11.91 M) for 12 hours, the green fluorescence intensity was shown to be increased, indicating that intracellular ROS was accumulated in the mitochondria of U-87MG cells. As indicated in Figure 5 a, the increased level of ROS after treatment of U-87MG cells with 5c derivative was significantly higher compared to the U-87MG unexposed negative cells (Figure 5a , $P < 0.01$). These results demonstrate that 5c induces growth inhibition and apoptosis by enhancing intracellular oxidative stress of U-87MG glioblastoma cells.

The increased caspase-3 activity in a 5c-induced apoptosis

The level of caspase-3 activity is considered a marker of apoptosis and is determined in the current study using the Caspase-3/CPP32 Fluorometric Assay Kit. After treatment of U-87MG cells with 11.91 μM 5c derivative for 24 hours, a significant increase in caspase 3 activation was observed compared to the unexposed negative U-87MG cells (Figure 5b, $P<0.01$). The increased caspase-3 activity suggested that the 5c-derivative-induced apoptosis might occur in a caspase-dependent manner.

Discussion

The aggressive and malignant trait of GBM, characterized by a tumor-invasive phenotype with tentacle-like protrusions, results in difficulties and inadequacies in complete surgical tumor removal (Shao et al., 2018). The therapeutic complications of GBM, along with chemotherapy resistance and chemotherapy-induced toxicity, underscore the need to develop more potent chemotherapeutic agents to target multiple molecular pathways, induce apoptosis, and suppress prosurvival signals in glioblastoma multiforme tumors (Smith et al., 2007). Accordingly, in the current study, the antineoplastic effects of the novel imidazoquinoline compound and its various derivatives were examined in human glioblastoma U-87MG cells. Based on data, the imidazoquinoline-5c derivative showed a potent inhibitory effect on glioblastoma cell growth, which was accompanied by remarkable induction of apoptosis and phosphatidylserine exposure. Furthermore, imidazoquinoline-5c derivatives induced cell cycle arrest, ROS generation and caspase-3 activation in glioblastoma cells. The cytotoxic effect of the 5c derivative was dose- and time-dependent with an IC_{50} of 11.91 μM after a 24-hours incubation. Based on data, the imidazoquinoline-5c derivative can selectively inhibit cell growth of U-87MG and showed minimal effects on normal skin cells of AGO1522. The antitumor effect of imidazoquinoline compounds has been studied exclusively in various cancer cells. Accordingly, imidazoquinolines were shown to induce dose-dependent toxicity on human (T24) and murine (MBT-2) bladder cancer cells and were accompanied by induction of apoptosis, production of cytokines, c-Myc down-regulation and reduction of bladder cells tumorigenesis (Smith et al., 2007). In addition, Gardiquimod as a TLR7 agonist has been shown to suppress proliferation and migration of BxPC3 pancreatic cancer cells, which have been implicated in the induction of apoptosis. It has been postulated that the expression levels of cell cycle mediators such as cyclin B1 and cyclin E and mediators of the apoptotic pathway such as Bcl2 and Bax are regulated by gardiquimod (Zou et al., 2015). It is well-documented that membrane changes and permeabilization of the cell membrane are essential events of the apoptosis process and accounts as a key feature of antitumor compounds(Happo et al., 2012). The data showed that treatment of the 5c derivative of U-87MG cells induced the percentage of early and late apoptotic cells, indicating the ability of 5c to increase the permeability of U-87MG cells. In support of our data, imidazoquinolines were shown to reduce cell viability and induce deoxyribonucleic acid fragmentation, leading to induction of apoptosis in RCC, which could occur through overexpression of TLR7. The ability of imidazoquinolines to suppress tumor growth and induce apoptosis has been demonstrated in metastatic RCC in the mouse model (Schwartz et al., 2009). Notably, the pro-apoptotic effect of imiquimod was investigated in various skin cancer cell types including melanoma and the results showed that imiquimod induced apoptosis via the mitochondrial pathway and Bcl-2-dependent cytochrome c to cytosolic translocation (Schön et al., 2004). Imiquimod has been shown to have anti-cancer effects on melanoma cells by promoting autophagy and sensitizing cancer cells to radiation treatment and chemotherapy and inducing immune responses (Cho et al., 2017). Imidazoquinoline was reported to decrease cell viability, induce apoptosis and cytokine production in transitional cell carcinoma cell lines, consistent with the antitumor effects thereof in the immunocompetent orthotopic mouse model (Smith et al., 2007). Our data showed that the 5c derivative affected the cell cycle distribution pattern to induce arrest in phase S and G2-M and to increase the percentage of cells in the sub-G1 fraction, which is thought to be a hallmark of apoptosis. The influence of imidazoquinoline compounds on cell cycle distribution has been reported in other cancer cells, as treatment of TRAMP-C2 mouse prostate cancer cells with imiquimod has been shown to induce cell cycle arrest in the G2/M phase and apoptosis in a mitochondria-dependent pathway (Han et al., 2013). It was shown that EAPB0203 and EAPB0503, which are structural analogues belonging to the imidazo[α-1,2]quinoxaline family of imiquimod, were able to induce apoptosis and cell cycle arrest in G2/M phase and cell growth in ATLL cells (EAPB0203) and CML cells (EAPB0503). Furthermore, EAPB0203 negatively regulated anti-apoptotic proteins such as c-IAP-1 and Bcl-xL and stabilized pro-apoptotic proteins such as p53 and p21 also activated the p38-MAPK pathway in malignant T cells (Moarbess et al., 2008). Additionally, EAPB0203 and EAPB0503 were shown to inhibit cell proliferation, block the cell cycle in G2 and M

phase, and induce apoptosis in A375 cells. Accordingly, treatment with EAPB0203 and EAPB0503 was associated with inhibition of polymerization of purified tubulin in a cell-free system and disruption of microtubule network organization at the cellular level in melanoma A375 cells, indicating the potent anti-microtubule activity of these compounds (Courbet et al., 2017). It is well-documented that caspase-3 is an activated protease mediates cleavage of key cellular proteins and execute death morphology (Porter and Jänicke, 1999). Our data showed that treatment of U-87MG cells with 5c derivative was associated with increased caspase-3 activity, suggesting that induction of apoptosis occurs in a caspase-dependent manner in U-87MG cells. It is also taken for granted that intracellular ROS is involved in the activation of many cellular signaling pathways and regulates processes involved in cell proliferation and differentiation. ROS-induced apoptosis involving mitochondria and death receptors has been demonstrated in various cancer cells. Accordingly, our data showed that the 5c derivative led to an accumulation of intracellular ROS in the mitochondria of U-87MG cells, suggesting that the 5c derivative-induced apoptosis in a ROS-dependent manner in U-87MG cells could occur. In support of our data, it was shown that ROS is produced after drug-induced intrinsic oxidative stress, which was associated with cytotoxic effects and inhibition of cell proliferation (Conklin, 2004). It is postulated that after ROS accumulation, the intrinsic mitochondrial apoptotic pathway is triggered and leads to disruption of mitochondrial membrane potential, cytochrome c release, caspase-9 activation and exchange of Bax/Bcl-2 ratios, which ultimately induce apoptosis in a target cell (Byun et al., 2009). The same method is proposed for imidazoquinolines-induced ROS accumulation, which could be followed by disruption of mitochondrial function and induction of the intrinsic apoptotic pathway. Accordingly, it was shown that the new amidino-substituted derivative of benzimidazo[α-1,2] quinolone inhibited the growth of HCT 116 colon cancer cells, probably by altering p53 gene expression, which could be triggered by DNA damage and oxidative stress. Imidazoquinolines have been shown to induce p53-dependent cell cycle arrest and apoptosis in both caspase-dependent and caspase-independent ways in HCT 116 cells. It is noteworthy that the quinoline derivative induced p53-independent G2-M arrest in SW620 cells, which are mutant p53 cells (Sedic et al., 2008).

In conclusion, our preliminary study demonstrated that the novel imidazoquinoline compound induced cell apoptosis and antiproliferative effects in glioblastoma U-87MG cells in a dose- and time-dependent manner. The effect of the 5c derivative was characterized by a subsequent increase in caspase-3 activity, accumulation of ROS and induction of cell cycle arrest in U-87MG cells. Further in vivo studies besides mechanistic investigations on the antiproliferative properties of imidazoquinoline compounds are needed to strengthen and validate the role of imidazoquinoline as a putative anticancer agent for glioblastoma chemoprevention.

Author contribution statement

All authors contributed to the study conception and design. All authors read and approved the final manuscript. Fatemeh Mostafavi Hosseini and Maryam Ashourpour contributed in methodology, data collection, data analysis and writing original draft. Salman Taheri contributed in material preparation and methodology. Masoumeh Tavakoli Yaraki and Siamak Salami contributed in review and editing. Zahra Shahsavari and Faranak Kazerouni contributed in supervision, project administration, writing, review and editing.

Acknowledgments

This work was supported by the Shahid Beheshti University of Medical Sciences, Faculty of Paramedical Sciences, Tehran, Iran [grant number: 11079]. This article has been extracted from the M.Sc. thesis written by Fatemeh Mostafavi Hosseini in Faculty of Paramedical Sciences, Shahid Beheshti University of Medical Sciences.

Ethics approval and consent to participate

Not applicable.

Conflicts of Interest

The authors declare that they have no conflict of interest.

References

Bazin HG, Bess LS, Livesay MT (2018). Synthesis and applications of imidazoquinolines: A Review. *Org Prep Proced Int*, **50**, 109-244.

Byun J-Y, Kim M-J, Eum D-Y, et al (2009). Reactive oxygen species-dependent activation of Bax and poly (ADP-ribose) polymerase-1 is required for mitochondrial cell death induced by triterpenoid pristimerin in human cervical cancer cells. *Mol Pharmacol*, **76**, 734-44.

Cho JH, Lee H-J, Ko H-J, et al (2017). The TLR7 agonist imiquimod induces anti-cancer effects via autophagic cell death and enhances anti-tumoral and systemic immunity during radiotherapy for melanoma. *Oncotarget*, **8**, 24932.

Conklin KA (2004). Cancer chemotherapy and antioxidants. *J Nutr*, **134**, 3201-4.

Courbet A, Bec N, Constant C, et al (2017). Imidazoquinoxaline anticancer derivatives and imiquimod interact with tubulin: Characterization of molecular microtubule inhibiting mechanisms in correlation with cytotoxicity. *PLoS One*, **12**, e0182022.

Elsakka A, Bary MA, Abdelzaher E, et al (2018). Management of glioblastoma multiforme in a patient treated with ketogenic metabolic therapy and modified standard of care: a 24-month follow-up. *Front Nutr*, **5**, 20.

Han J-H, Lee J, Jeon S-J, et al (2013). In vitro and in vivo growth inhibition of prostate cancer by the small molecule imiquimod. *Int J Oncol*, **42**, 2087-93.

Hanif F, Muzaffar K, Perveen K, et al (2017). Glioblastoma multiforme: a review of its epidemiology and pathogenesis through clinical presentation and treatment. *Asian Pac J Cancer Prev*, **18**, 3.

Happo L, Strasser A, Cory S (2012). BH3-only proteins in apoptosis at a glance. *J Cell Sci*, **125**, 1081-7.

Hu Z, Mi Y, Qian H, et al (2020). A potential mechanism of

temozolomide resistance in Glioma–Ferroptosis. *Front Oncol*, **10**, 897.
Huang B, Zhang H, Gu L, et al (2017). Advances in immunotherapy for glioblastoma multiforme. *J Immunol Res*, **2017**.
Kauffman EC, Liu H, Schwartz MJ, et al (2012). Toll-like receptor 7 agonist therapy with imidazoquinoline enhances cancer cell death and increases lymphocytic infiltration and proinflammatory cytokine production in established tumors of a renal cell carcinoma mouse model. *J Oncol*, **2012**.
Moarbess G, El-Hajj H, Kfoury Y, et al (2008). EAPB0203, a member of the imidazoquinoxaline family, inhibits growth and induces caspase-dependent apoptosis in T-cell lymphomas and HTLV-I–associated adult T-cell leukemia/lymphoma. *Blood J Am Soc Hematol*, **111**, 3770-7.
Porter AG, Jänicke RU (1999). Emerging roles of caspase-3 in apoptosis. *Cell Death Differ*, **6**, 99-104.
Schön MP, Wienrich BG, Drewniok C, et al (2004). Death receptor-independent apoptosis in malignant melanoma induced by the small-molecule immune response modifier imiquimod. *J Invest Dermatol*, **122**, 1266-76.
Schwartz MJ, Liu H, Hwang DH, et al (2009). Antitumor effects of an imidazoquinoline in renal cell carcinoma. *Urology*, **73**, 1156-62.
Sedic M, Poznic M, Gehrig P, et al (2008). Differential antiproliferative mechanisms of novel derivative of benzimidazo [1, 2-α] quinoline in colon cancer cells depending on their p53 status. *Mol Cancer Ther*, **7**, 2121-32.
Shao M, He Z, Yin Z, et al (2018). Xihuang pill induces apoptosis of human glioblastoma U-87 MG cells via targeting ROS-mediated Akt/mTOR/FOXO1 pathway. *Evid-Based Compl Alt*, **2018**.
Shergalis A, Bankhead A, Luesakul U, et al (2018). Current challenges and opportunities in treating glioblastoma. *Pharmacol Rev*, **70**, 412-45.
Smith EB, Schwartz M, Kawamoto H, et al (2007). Antitumor effects of imidazoquinolines in urothelial cell carcinoma of the bladder. *J Urol*, **177**, 2347-51.
Smith KJ, Hamza S, Skelton H (2003). The imidazoquinolines and their place in the therapy of cutaneous disease. *Expert Opin Pharmacother*, **4**, 1105-19.
Vacchelli E, Galluzzi L, Eggermont A, et al (2012). Trial watch: FDA-approved Toll-like receptor agonists for cancer therapy. *Oncoimmunology*, **1**, 894-907.
Zou BB, Wang F, Li L, et al (2015). Activation of Toll-like receptor 7 inhibits the proliferation and migration, and induces the apoptosis of pancreatic cancer cells. *Mol Med Rep*, **12**, 6079-85.